Nicola Michailow

Generalized Frequency Division Multiplexing
Transceiver Principles

Beiträge aus der Informationstechnik

Mobile Nachrichtenübertragung
Nr. 77

Nicola Michailow

Generalized Frequency Division Multiplexing Transceiver Principles

VOGT

Dresden 2015

Bibliografische Information der Deutschen Nationalbibliothek
Die Deutsche Nationalbibliothek verzeichnet diese Publikation in der Deutschen Nationalbibliografie; detaillierte bibliografische Daten sind im Internet über http://dnb.dnb.de abrufbar.

Bibliographic Information published by the Deutsche Nationalbibliothek
The Deutsche Nationalbibliothek lists this publication in the Deutsche Nationalbibliografie; detailed bibliographic data are available on the Internet at http://dnb.dnb.de.

Zugl.: Dresden, Techn. Univ., Diss., 2015

Die vorliegende Arbeit stimmt mit dem Original der Dissertation „Generalized Frequency Division Multiplexing Transceiver Principles“ von Nicola Michailow überein.

Gesetzt vom Autor

ISBN 978-3-938860-94-6

Jörg Vogt Verlag
Niederwaldstr. 36
01277 Dresden
Germany

Phone: +49-(0)351-31403921
Telefax: +49-(0)351-31403918
e-mail: info@vogtverlag.de
Internet : www.vogtverlag.de

TECHNISCHE UNIVERSITÄT DRESDEN

Generalized Frequency Division Multiplexing Transceiver Principles

Nicola Michailow

der Fakultät Elektrotechnik und Informationstechnik
der Technischen Universität Dresden

zur Erlangung des akademischen Grades eines

Doktoringenieurs
(Dr.-Ing.)

genehmigte Dissertation

Vorsitzender:	Jun.-Prof. Dr.-Ing. K. Jamshidi		
Gutachter:	Prof. Dr.-Ing. Dr. h.c. G. Fettweis	Tag der Einreichung:	02.02.2015
	Prof. Dr. Sci. (EE) M. Renfors	Tag der Verteidigung:	09.07.2015

Abstract

Despite the great success of orthogonal modulation schemes in state-of-the-art communication systems, their lack of flexibility is prohibitive for application in future 5G cellular systems. In 2009, the initial concept of a novel modulation scheme named generalized frequency division multiplexing (GFDM) was proposed. It represents a new perspective on filtered multicarrier transmission with more degrees of freedom than classical OFDM or SC-FDE transmission and is capable to address the specific requirements of 5G application scenarios. This work develops the foundations of GFDM modulation and demodulation and analyzes how characteristic parameters influence the properties of the waveform.

The first part of this work explores the basic GFDM transmitter and receiver. For this purpose, the terminology around the block structure of GFDM is clarified and based on these definitions, the GFDM baseband processing, i.e. signal generation and matched filter reception, is described from multiple perspectives, including a low complexity model. The bit error rate performance is analyzed for multiple channel conditions, analytically and through simulations.

The second part of this work treats enhanced receiver structures. The linear zero forcing and minumum mean squared error receiver are derived for GFDM and their error rate performance is evaluated. Subsequently, two non-linear receivers are developed. A matched filter in combination with successive interference cancellation as well as an adaptive minumum mean squared error structure are analyzed in terms of bit error rates. Moreover, GFDM is considered in combination with channel coding for different channel conditions. Lastly, based on the number of complex valued multiplications required for an implementation, the computational complexity of the different transmitter and receiver algorithms is compared.

The third part of this work focuses on engineering the GFDM waveform according to specific requirments. This analysis starts with an investigation of the spectral properties in dependence of the various available degrees of freedom. The focus is then shifted to multi-user interference and multi-system coexistence, particularly in the case of frequency misalignment. The peak-to-average power ratio of GFDM is analyzed for multicarrier and single-carrier configurations. The work is concluded by the derivation of specific sets of parameters for the GFDM waveform that enable to address envisioned 5G application scenarios.

Contents

Chapter 1

Introduction

Modern society highly depends on mobile communication. Starting with the first generation (1G) of cellular systems, which in the 1980s provided the basic means for analogue voice transmission, cellular networks have evolved during the past decades. Until today, communication experienced a paradigm shift in 'how' and 'when': It has become a personal service, rather than being constrained to fixed locations.

Each step in the evolution has had its own innovation. From the second generation (2G) on, all subsequent cellular systems have employed digital modulation because it offers numerous advantages like higher system capacity, increased battery life of the mobile terminals and a better Quality of Service (QoS). And although not completely intended, 2G revolutionized the way people communicate with the Short Message Service (SMS). The third generation (3G) enabled Internet access with mobile terminals and data rates not far below wired solutions of that time. The emergence of smartphones, handheld devices with unprecedented processing power, equipped with high resolution screens and cameras, has turned the users from media consumers into content providers. This trend has guided the fourth generation (4G) towards even higher data rates and throughput, in order to keep pace with the requirements imposed by social networks and cloud-based services.

Up to now, the progress of the mobile systems has been focused on increasing the data rates, throughput, user experience and coverage. However, higher throughput alone will not suffice to address the challenges foreseen for the fifth generation (5G) of cellular networks. While the classical bitpipe communication will still have an integral role in the future, communication with low latency has been identified as an essential ingredient that will facilitate new services such as the Tactile Internet [Fet14]. Moreover, the Internet of Things (IoT) [AIM10] will give rise to large scale sensor and actuator networks. A huge set of use cases that can be summarized by the term machine type communication (MTC) [WJK+14] requires support of massive wireless connectivity.

From these use cases, the demand for a reduced latency, minimal spectral emmissions, fragmented spectrum allocation and relaxed synchronization can be derived. Hence 5G

needs to be extremely flexible and this requirement also reflects on the properties of the physical layer (PHY) modulation scheme that will be employed.

1.1 Flexible Multicarrier Modulation

The history of filtered multicarrier systems can be traced back to the second half of the 1960ies, when Chang and Saltzberg independently invented a technique for efficient parallel data transmission [Cha66, Sal67]. Since that time, one particular derivate of the proposed scheme, namely orthogonal frequency division multiplexing (OFDM) [Bin90], gained enormous popularity in practical applications and scientific community. Countless efforts have been put into researching OFDM and, as a consequence, a vast amount of knowledge is available on this topic [BS99, HB08, Gol05, Tse05]. Today, the physical layer of many wired and wireless communication standards is based on OFDM. Prominent examples include dynamic subscriber line (DSL), power line communication (PLC), IEEE 802.11 specifications (802.11), Long Term Evolution (LTE), terrestrial digital video broadcasting (DVB-T) and terrestrial integrated services digital broadcasting (ISDB-T), just to name the main standards. The overwhelming success of OFDM is partly due to the simple structure of transmitter and receiver as well as to its ability to efficiently cope with frequency-selective channels. These properties allow keeping the power consumption in mobile terminals low. However, especially in wireless communications, another important aspect is the limited availability of frequency resources. A prominent alternative air interface that can address spectral shaping is single-carrier with frequency domain equalization (SC-FDE) [FABSE02].

Despite the great success of OFDM in state-of-the-art communication systems, the scheme has several shortcomings that are prohibitive for its application in 5G systems. The cyclic prefix (CP) [Gol05] and an appropriately chosen subcarrier spacing, which are necessary to make OFDM effective in frequency-selective channels, impede the use of short OFDM symbols and hence prevent achieving a low latency. Moreover, due to the unfavorable out-of-band properties of the waveform, an efficient use of fragmented spectrum resources necessitates additional adaptive filtering. Lastly, OFDM is sensitive to frequency misaligments between transmitter and receiver, which requires the use of sophisticated synchronization procedures and consumes energy.

In 2009, the initial concept of a novel modulation scheme named generalized frequency division multiplexing (GFDM) was proposed [FKB09]. It represents a new perspective on filtered multicarrier transmission with more degrees of freedom than classical OFDM or SC-FDE and is capable to address the specific aspects of 5G that have been previously discussed.

1.2 Outline

This work develops the foundations of GFDM modulation and demodulation and analyzes the dependency of the scheme on its characteristic parameters. It aims to answer the question, in which cases a non-orthogonal waveform should be favored over established orthogonal alternatives and show why. For this purpose, a multitude of aspects are studied, including the time-frequency structure of the signal, basic waveform generation and reception aspects, advanded linear and also non-linear receiver algorithms as well as error correction coding. Moreover, the spectral properties, implementation complexity and peak-to-average power ratio (PAPR) behavior are accounted for and relevant transmission scenarios are kept in mind. The findings are presented in the following structure:

Chapter 2 builds a foundation for the subsequent analyses. It explores common concepts for modelling wireless channel, gives an overview of state-of-the-art filtered multicarrier systems and reviews the details of OFDM, SC-FDE and filter bank multicarrier (FBMC) modulation in particular. Moreover, the chapter introduces selected 5G transmission scenarios.

Chapter 3 treats the basic GFDM transmitter and receiver. First, the terminology around the block structure of GFDM is clarified. Based on these definitions, the GFDM baseband processing, i.e. signal generation and matched filter reception, is described from multiple perspectives, including a low complexity model. The chapter is concluded by bit error rate performance analysis for multiple channel conditions, analytically and through simulations.

Chapter 4 presents enhanced receiver structures. First, the linear zero forcing and minumum mean squared error receiver are derived for GFDM and their error rate performance is evaluated. Next, two non-linear receivers are developed. A matched filter in combination with successive interference cancellation as well as an adaptive minumum mean squared error structure are analyzed in terms of bit error rates. Moreover, GFDM is considered in combination with channel coding for different channel conditions. Lastly, based on the number of complex valued multiplications required for an implementation, the computational complexity of the different transmitter and receiver algorithms is compared.

Chapter 5 focuses on engineering the GFDM waveform according to specific requirments. The analysis starts with an investigation of the spectral properties in dependence the various available degrees of freedom. Then the focus is shifted to multi-user interference and multi-system coexistence, particularly in the case of frequency misalignment. The peak-to-average power ratio of GFDM is analyzed for multicarrier and single-carrier configurations. The chapter is concluded by the derivation of specific sets of parameters for the GFDM waveform that enable to address the envisioned 5G application scenarios.

Finally, in Chapter 6 conclusions are drawn and perspectives for future work are outlined.

Chapter 2

Fundamentals

Before the specifics of generalized frequency division multiplexing (GFDM) can be addressed in the following chapters, a collection of relevant basic principles and concepts will be provided. First, a set of mathematical models for the wireless channel is presented, which is an essential prerequisite when analyzing the error rate performance of a communication system analyticaly and through simulations. The second part of the chapter provides an overview of filtered multicarrier systems. Various modulation schemes are put in relation to each other and the mathematical baground for three selected waveforms is provided. Lastly, three relevant envisioned transmission scenarios for future cellular systems are outlined and serve as motivation to investigate techniques beyond the state-of-the-art.

2.1 Modelling the Wireless Channel

Proper modeling of the transmission channel is essential when investigating communication systems, as it enables to analyze the performance with analytical tools and through simulation. There are various ways to define a channel between transmitter and receiver [Nus10, pp. 5]. The set of physical aspects captured in such a model highly depends on the purpose of the investigation. In the context of this work, the wireless channel that accounts for the signal propagation properties through the physical medium is particularly relevant, while the behaviour of antennas and circuits is neglected. In the following, the four wireless channel models that are depicted in Figure 2.1 are briefly introduced, i.e. additive white Gaussian noise (AWGN), multipath propagation, Rayleigh fading, and Rayleigh multipath block fading. Other models like Doppler fading or Rice fading are out of the scope of this work.

Additive White Gaussian Noise: The main purpose of the AWGN channel model is to capture noise from various sources, e.g. thermal noise of circuits and components,

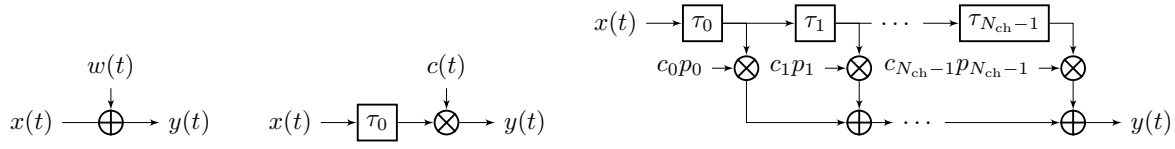

(a) AWGN **(b)** Rayleigh fading **(c)** Multipath block fading

Figure 2.1: Block diagrams of selected channel models.

cosmic radiation and other noise sources. Distortions to the transmitted signal are not considered in the mathematical representation

$$y(t) = x(t) + w(t), \tag{2.1}$$

where $x(t)$ and $y(t)$ are the signals at the input and the output of the AWGN channel respectively and $w(t)$ is the additive noise term

$$w(t) = w_{\mathrm{re}}(t) + jw_{\mathrm{im}}(t), \quad w_{\mathrm{re}}(t) \sim \mathcal{N}\left(0, \frac{1}{2}\sigma_w^2\right), w_{\mathrm{im}}(t) \sim \mathcal{N}\left(0, \frac{1}{2}\sigma_w^2\right) \tag{2.2}$$

is a complex random variable with zero mean and variance σ_w^2 with Gaussian distribution of the real and imaginary part. Subsequent realizations of noise are uncorrellated, which reflects in a constant noise power density N_0 and hence the noise is referred to as 'white'. The relation to the variance of the Gaussian distribution is given by $\sigma_w^2 = N_0/2$. Putting N_0 in relation to the energy E_b that is required to transmit a single bit yields the signal-to-noise ratio (SNR) per bit E_b/N_0, which is a paremeter that compares the energy of the useful signal to the energy of the noise. Lastly, a block diagram of the AWGN model can be found in Figure 2.1(a).

Multipath Propagation: When electromagnetic waves pass through a physical medium, they face effects like reflection, inflection and dispersion. As a consequence, multiple copies of a transmitted signal can reach the receiver on different propagation paths. Each path contributes with an individual delay, angle of arrival and attenuation. These properties are characterized by a power delay profile (PDP) p_i, $i = 0, \ldots, N_{\mathrm{ch}} - 1$, where N_{ch} is the total number of signal paths observed at the receiver. The PDP is obtained by evaluating the autocorrelation function of the equivalent low-pass time-variant impulse response of the channel [Gol05, pp.82-87]. For a set of propagation delays $\{\tau_i\}$, the signal at the channel output can be written as

$$y(t) = \sum_{i=0}^{N_{\mathrm{ch}}-1} p_i x(t - \tau_i). \tag{2.3}$$

It may occur, that multiple copies of the signal overlap in a way that makes certain frequency components subject to strong attenuation. This property is characterized by the coherence bandwidth B_{c} of the channel. It is a statistical measure of the bandwidth

over which the frequency components of the signal are subject to experience comparable fading. As a rule of thumb, it can be related to the root mean square (rms) delay spread

$$\tau_{\text{rms}} = \sqrt{\frac{\sum_i \left((\tau_i - \bar{\tau})^2 p_i\right)}{\sum_i (\tau_i - \bar{\tau})}}, \bar{\tau} = \frac{\sum_i (\tau_i p_i)}{\sum_i \tau_i} \tag{2.4}$$

and the frequency correlation between the input and the output of the channel [R+96, pp.163-164]. The relation is given as

$$B_{\text{c}} \approx \begin{cases} \frac{1}{5\tau_{\text{rms}}} & \text{for 50 \% correlation} \\ \frac{1}{50\tau_{\text{rms}}} & \text{for 90 \% correlation.} \end{cases} \tag{2.5}$$

Rayleigh Fading: There is a second aspect of multipath propagation. When the electromagnetic wave is scattered in the close proximity of the receiver, the different paths can produce delays below the resolution capabilities of the system. In that case, all uncorrelated scatters are assigned a single delay τ_0. Moreover, it is assumed that all angles of arrival are equally probable, that each path is received on average with the same power and that there is no line-of-sight connection. The superposition of all scatterers leads to a time variant transmission, i.e. Rayleigh fading, which can be modeled as multiplication of the channel input with a random variable $c(t) = c_{\text{re}}(t) + jc_{\text{im}}(t)$. The channel output can be formulated as

$$y(t) = c(t)x(t - \tau_0), \quad c_{\text{re}}(t) \sim \mathcal{N}\left(0, \frac{1}{2}\sigma_c^2\right), c_{\text{im}}(t) \sim \mathcal{N}\left(0, \frac{1}{2}\sigma_c^2\right) \tag{2.6}$$

and as a result, $\angle c(t)$ follows a uniform distribution and $|c(t)|$ follows a Rayleigh distribution. Rayleigh fading can be modelled according to the diagram in Figure 2.1(b).

Rayleigh Multipath Block Fading: In this wireless channel model, the properties of AWGN, multipath propagation and Rayleigh fading are combined. Additionally, the propagation delays are assumed constants and the signal is considered to be partitioned into independent blocks, which are provided sequentially to the input of the channel. If the duration of the blocks is short, it can be assumed that $c(t) = c$, i.e. the Rayleigh fading is constant for that period. The resulting Rayleigh multipath block fading model can be mathematically described as the convolution

$$y(t) = h(t) * x(t) + w(t) \tag{2.7}$$

of the transmitted signal $x(t)$ with a channel impulse response

$$h(t) = \sum_{i=0}^{N_{\text{ch}}-1} c_i p_i \delta(t - \tau_i). \tag{2.8}$$

A finite impulse response (FIR) representation of Rayleigh multipath block fading is given in Figure 2.1(c).

Because of $h(t)$, the SNR per bit is altered. To allow a fair comparison with the AWGN case, the expression [Pro08, pp. 830-891]

$$\overline{E_b}/N_0 = \sum_i \sigma_c^2 p_i^2 \frac{E_b}{N_0} \tag{2.9}$$

will denote the effective SNR in the Rayleigh multipath block fading model.
In a digital communication system that operates at a sampling period T_s, the continuous time variable t can be replaced by the discrete time $n = t/T_\mathrm{s}$, leading to

$$h[n] = \sum_i c_i p_i \delta[n - \eta_i]. \tag{2.10}$$

with the integer tap delays η_i. Collecting the signal samples of channel input, channel output, channel impulse response and noise in the respective vectors $\vec{x} = (x[n])_{n=0,\ldots,N-1}$, $\vec{y} = (y[n])_{n=0,\ldots,N-1}$, $\vec{h} = (h[n])_{n=0,\ldots,N-1}$ and $\vec{w} = (w[n])_{n=0,\ldots,N-1}$ allows to formulate the transmission as

$$\vec{y} = \vec{h} * \vec{x} + \vec{w}. \tag{2.11}$$

2.2 Filtered Multicarrier Systems

Recent trends in research community indicate efforts towards new waveforms [WJK+14], which can be related to the original proposal of Chang and Saltzberg. An overview of filtered multicarrier systems is given in Figure 2.2(a). The diagram shows two categories, the block-based and the continuous transmission schemes. One of the main properties of the well established orthogonal frequency division multiplexing (OFDM) scheme is that the signal is modulated by dividing a given frequency resource into a large number of narrowband slices. A similar partitioning is done in single-carrier with frequency domain equalization (SC-FDE), however in this case a time resource is divided. Based on these two schemes, single-carrier frequency division multiplexing (SC-FDM) can be considered a way of slicing both dimensions at the same time. SC-FDM can be seen either as the concatenation of several OFDM symbols in time or as the concatenatation of several SC-FDE carriers in frequency. Such a two dimensional grid is the foundation for GFDM [MMG+14], which can be seen as a further evolution that is achieved by additional circular filtering and windowing. In the context of this work, these four schemes will be most relevant and OFDM and SC-FDE will serve as a reference when evaluating the performance of GFDM.

The filter bank multicarrier (FBMC) scheme [FB11, BNW+10, IHSRR06], which is in the focus of several research projects [PHY, EMP, MET], poses an interesting alternative to OFDM. It is also based on subcarrier filtering. However, in contrast to GFDM a block structure is not followed in FBMC. There are two major variations of the scheme. The first one is obtained by replacing regular quadrature amplitude modulation (QAM) with

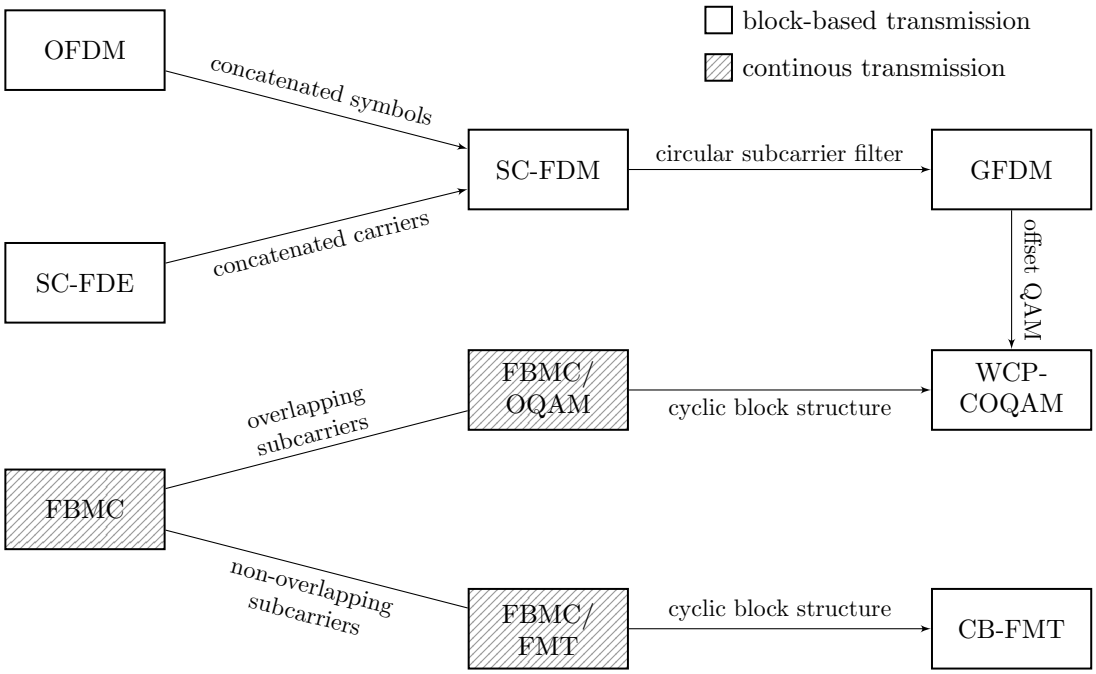

(a) General overview.

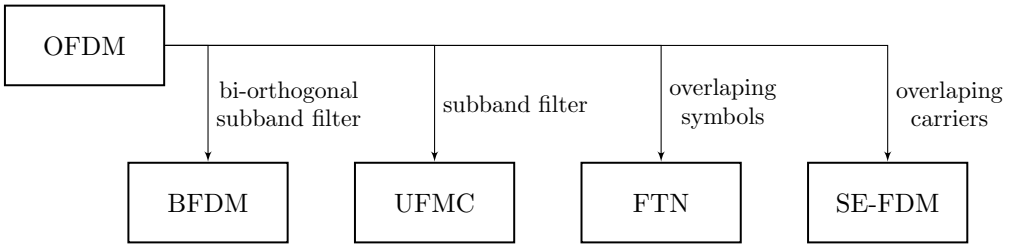

(b) OFDM based schemes.

Figure 2.2: The landscape of filtered multicarrier systems.

offset quadrature amplitude modulation (OQAM). This enables to maintain orthogonality in the real domain, when overlapping pulse shaped subcarriers would otherwise cause interference among themselves. The other direction in which FBMC has been developed is filtered multi tone (FMT) [CEOC00], which requires to increase the distance between subcarriers in the frequency domain to avoid interference.

A connection between QAM-based GFDM and FBMC-OQAM can be drawn from two perspectives. One option is to introduce a cyclic block structure which removes filtering tails and leads to the cyclic offset QAM with windowed CP (WCP-COQAM) technique [LS14]. Then, the offset between real and imaginary part in the OQAM signal needs to be eliminated. Alternatively, GFDM can be modified to operate with OQAM modulation [MF15, GMM$^+$15] and filtering tails can be purposely introduced at the beginning and at the end of a signal burst. On the other hand, extending FBMC-FMT with a cyclic block structure yields cyclic block filtered multitone (CB-FMT) [Ton13], which is already a very close relative to GFDM. The remaining difference is the fact that GFDM is purposely de-

signed to tolerate interference between overlapping subcarriers, while in CB-FMT only the special case of non-overlapping subcarriers is used.
In Figure 2.2(b), several schemes that can be derived directly from OFDM are presented. The faster than Nyquist signalling (FTN) is created by partially overlapping OFDM symbols along the time axis [ARO13]. In analogy, spectrally efficient frequency division multiplexing (SE-FDM) is the result of a similar procedure applied along the frequency axis, i.e. to the subcarriers of OFDM [KCRD09]. For example, when signaling with sinc pulses, both methods allow a compression of up to approximately 25% [Maz75, KCRD09] without loss in minimum Euclidian distance. Consequently, compared to OFDM, more data can be packed into a given time-frequency resource. This property comes at the cost of self-interference, which makes sophisticated receiver structures necessary. The two other schemes, bi-orthogonal frequency division multiplexing (BFDM) and universally filtered multicarrier (UFMC), target improving the out-of-band properties of OFDM. The core property of UFMC is a subband filter that is applied across a continuous set of subcarriers in the system. However, the performance of the scheme suffers, when there is a small time misalignment between users, because unlike OFDM, there is no cyclic prefix (CP) [VWS+13]. The special feature of BFDM [BDH99] is its bi-orthogonal filter that is used for reception, which relates the scheme directly to the theory of Gabor signaling.
Until today, from all different kinds of filtered multicarrier systems, only a subset of orthogonal systems has found a relevant position in timely communication standards. Historically, orthogonality has been favored, because it facilitates simple algorithms and implementation with low computational complexity. However advances in microelectronics during the past years have lifted this concern. Processing elements and memory chips can now easily handle more complex algorithms, which allows to trade complexity in favor of improving other properties of the modulation scheme.
In the following, the mathematical background of three selected schemes will be reviewed.

2.2.1 Orthogonal Frequency Division Multiplexing

A major advantage of OFDM [HB08, BS99] comes with the multicarrier nature of the scheme. In a multipath fading scenario, the wireless channel is divided into low-rate subchannels. If the bandwidth of the individual subchannels is smaller than coherence bandwidth, each subchannel can be considered frequency flat. In combination with a cyclic prefix, this property allows simple channel equalization by zero-forcing in frequency domain. Further, OFDM benefits from orthogonality, which makes subcarriers and symbols independent of each other. The transmitter and receiver can be efficiently implemented in hardware with the fast Fourier transform (FFT) algorithm. The drawbacks of OFDM include a high sensitivity to frequency offsets between transmitters and receivers e.g. caused by Doppler spread, strong spectral leakage as well as unfavorable peak-to-average power ratio (PAPR) properties due to the multicarrier nature of the signal.
A block diagram depicting a basic OFDM transceiver chain is presented in Figure 2.3.

From a mathematical point of view, a significant property of OFDM is the definition of transmit data in frequency domain. Let $\vec{d} = (d_n)_{n=0,\dots,N-1}$ be a set of complex-valued data symbols. Then the transmit samples $\vec{x}$ can be obtained through inverse discrete Fourier transform (IDFT) according to

$$\vec{x} = \mathbf{W}_N^{\mathrm{H}} \vec{d}, \tag{2.12}$$

where $\mathbf{W}_N = \frac{1}{\sqrt{N}} (w_{n_1,n_2})$ with $w_{n_1,n_2} = \exp\left(j2\pi \frac{n_1 n_2}{N}\right)$ and $n_1, n_2 \in \{0, 1, \dots, N-1\}$ is a $N \times N$ Fourier matrix. While this way of modulation makes the data symbols orthogonal, it inherently also imposes a rectangular pulse shape to the time domain signal. Consequently, the spectral properties are determined by the $\sin(x)/x$ function and as a result, OFDM exhibits disadvantageous properties regarding out-of-band radiation.
Moreover, to avoid losing orthogonality when the signal passes through a time dispersive channel, OFDM can be used in combination with a cyclic prefix of length $T_{\mathrm{CP}} \leq T_{\mathrm{ch}}$. This translates to $N_{\mathrm{CP}} \leq N_{\mathrm{ch}}$ in digital domain and the prefixing operation can be expressed as

$$\vec{\tilde{x}} = \mathbf{P}\vec{x}, \ \mathbf{P} = \left(\begin{array}{c|c} \mathbf{0} & \mathbf{I}_{N_{\mathrm{CP}}} \\ \hline & \mathbf{I}_N \end{array} \right), \tag{2.13}$$

yielding the extended vector $\vec{\tilde{x}}$. Transmission through a wireless channel can be then modeled as

$$\vec{\tilde{y}} = \tilde{\mathbf{H}}\vec{\tilde{x}} + \vec{\tilde{w}}, \tag{2.14}$$

where $\vec{\tilde{y}}$ is the received counterpart of $\vec{\tilde{x}}$, $\tilde{\mathbf{H}}$ is a $(N + N_{\mathrm{CP}}) \times N$ convolution matrix with band-diagonal structure derived from the channel impulse response $\vec{h}$ and $\vec{\tilde{w}} \sim \mathcal{CN}(\mathbf{0}, \sigma_w^2 \mathbf{I}_{N+N_{\mathrm{CP}}})$ denotes AWGN. Assuming perfect time and frequency synchronization, the CP can be stripped from the signal at the receiver, which allows to replace the channel matrix the $N \times N$ circular convolution matrix $\mathbf{H}$ and simplify the transmission model to

$$\vec{y} = \mathbf{H}\vec{x} + \vec{w}. \tag{2.15}$$

If $\vec{h}$ is available at the receiver, zero-forcing (ZF) channel equalization can be performed according to

$$\vec{z} = \mathbf{H}^{-1}\vec{y} \tag{2.16}$$

and lastly, the data symbols are recovered with the discrete Fourier transform (DFT) operation

$$\hat{\vec{d}} = \mathbf{W}_N \vec{z}. \tag{2.17}$$

In the special case of ZF equalization, the procedure can be performed without matrix inversion by taking advantage of the fact that $\mathbf{H}$ is a circulant matrix [Bin90], which is diagonalized by the DFT, i.e.

$$\mathbf{H} = \mathbf{W}_N^{\mathrm{H}} \mathbf{\Lambda} \mathbf{W}_N, \quad \mathbf{\Lambda} = \mathrm{diag}\left(\mathbf{W}_N \vec{h}\right) \tag{2.18}$$

contains only diagonal elements. Here diag(·) denotes a matrix with the vector (·) on its diagonal and zeros elsewere. The equalization process can be combined with the demodulation and rewritten as

$$\vec{\hat{d}} = \left[\mathrm{diag}\left(\mathbf{W}_N \vec{h}\right)\right]^{-1} \mathbf{W}_N \vec{y}. \tag{2.19}$$

Due to the special structure of the channel matrix, the inversion of $\mathrm{diag}\left(\mathbf{W}\vec{h}\right)$ effectively requires the multiplication of a single coefficient for each data symbol. The drawback of ZF equalization is the potential amplification of the AWGN term at weak carriers in $\vec{y}$.

2.2.2 Single-Carrier with Frequency Domain Equalization

The SC-FDE modulation scheme is sometimes also referred to as 'precoded OFDM' with the main difference that the data symbols are defined in time domain instead of frequency domain. Consequently, while in OFDM each data is allocated to a small bandwidth and long time duration, in SC-FDE chunks with large bandwidth and short duration are used instead, which is relevant when considering different channel models. The scheme is attractive for cellular uplink transmission, because it offers significantly better PAPR properties compared to OFDM. This property will be addressed in Section 5.3. Moreover, SC-FDE allows to shift part of the computational complexity from the transmitter to the receiver.
A block diagram of the transceiver is given in Figure 2.4. The precoding in SC-FDE can be written as multiplication of the transmit data vector $\vec{d}$ with a Fourier matrix $\mathbf{W}_N$, which then cancels out with the IDFT operation in the transmitter described by (2.12). This leads to the trivial expression

$$\vec{x} = \mathbf{W}_N^{\mathrm{H}} \left(\mathbf{W}_N \vec{d}\right) = \vec{d}, \tag{2.20}$$

that denotes the entire SC-FDE modulation process. Note that the spectral properties of the signal are determined by the transmit filter that is used for digital-to-analog (D/A) conversion or subsequent radio frequency (RF) filtering. As the name suggests, channel equalization is performed in frequency domain, which requires to add a CP as it is done for OFDM. The transmission model and equalization process remain the same as given in (2.15) and (2.16). But when the SC-FDE demodulator

$$\vec{\hat{d}} = \mathbf{W}_N^{\mathrm{H}} \left[\mathrm{diag}\left(\mathbf{W}_N \vec{h}\right)\right]^{-1} \mathbf{W}_N \vec{d} \tag{2.21}$$

is compared to the OFDM counterpart (2.19), it can be observed that the IDFT that was saved in the SC-FDE transmitter has effectively been shifted to the receiver side.
Lastly, a generalization of the concept will be useful in the following chapters. While OFDM is a scheme that strictly employs frequency division and SC-FDE follows strict time division, the combination of both schemes will be further referred to as SC-FDM.

The concept is illustrated in Figure 2.5, where the main idea is to align K SC-FDE signals adjacent in frequency. Each signal carries the data $\vec{d}_k$, $k = 0, \ldots, K-1$ and is mapped to a certain frequency resource through simple multiplication with a complex oscillation $\vec{w}_k = \exp\left(-j2\pi\frac{k}{K}n\right)$. The resulting waveform is similar to the individual subcarriers in OFDM, but with the difference that each carrier carries multiple data symbols. When the carrier signals are assigned to different users, this scheme is known as single-carrier frequency division multiple access (SC-FDMA), the multiple access scheme used in the uplink of Long Term Evolution (LTE) [3GP10b].

2.2.3 Filter Bank Multicarrier

There are several subtypes of FBMC modulation, which have in common a pulse shaping of the subcarriers in the system. Unlike the rectangular function in OFDM, the filter in FBMC spans over multiple symbol periods. While this allows to control the out-of-band properties of the waveform, it can create self-interference between subcarriers and symbols of the system and also adds to the latency of the transmission. To avoid the interference, real and imaginary part of the data symbols can be seperated and modulated with an offset in time and frequency. This technique is known as OQAM modulation and allows to avoid inter-symbol interference (ISI) and inter-carrier interference (ICI).
Consider the FBMC/OQAM [IVSR10, Sti10] system depicted in Figure 2.6. Let $\vec{d}$ be a complex vector containing $N = KM$ QAM modulated data symbols and $\vec{q}$ be its OQAM modulated counterpart, where K and and M the number of subcarriers and subsymbols in the system. Both vectors can be interpreted as a concatenation of K subcarrier data vectors, i.e. $\vec{d} = (\vec{d}_k^{\mathrm{T}})_{k=0,\ldots,K-1}^{\mathrm{T}}$ and $\vec{q} = (\vec{q}_k^{\mathrm{T}})_{k=0,\ldots,K-1}^{\mathrm{T}}$, which allows to formulate the QAM-to-OQAM conversion as

$$\vec{d}_k = \begin{pmatrix} \ldots & d_{k,m} & d_{k,m+1} & \ldots \end{pmatrix} \tag{2.22}$$

$$\vec{q}_k = \begin{cases} \begin{pmatrix} \ldots & \Re\{d_{k,m}\} & \Im\{d_{k,m}\} & \Re\{d_{k,m+1}\} & \Im\{d_{k,m+1}\} & \ldots \end{pmatrix}, & k \text{ even} \\ \begin{pmatrix} \ldots & \Im\{d_{k,m}\} & \Re\{d_{k,m}\} & \Im\{d_{k,m+1}\} & \Re\{d_{k,m+1}\} & \ldots \end{pmatrix}, & k \text{ odd.} \end{cases} \tag{2.23}$$

In $\vec{q}$, the real and imaginary part of the data symbols are separated which doubles the number of elements and leads to a relative offset of one half symbol period between in-phase (I) and quadrature-phase (Q). Additionally, there is a phase offset between odd and even subcarriers which results in an alternating $\Re(\cdot)$ and $\Im(\cdot)$ pattern. The vector $\vec{q}$ is passed to the synthesis filter bank, which applies a filter to the data symbols on each subcarrier. The individual subcarrier filters are based on a low-pass prototype filter response $\vec{g}_{\mathrm{s}}$ with overlapping factor L_M, which denotes its length in subsymbol periods. Using a real-valued, symmetric prototype filter, the filtering can be implemented efficiently in time domain with a polyphase network as described in [BNW+10, VIS+09]. The signal is then transmitted through the wireless channel without adding a CP. On the receiver side,

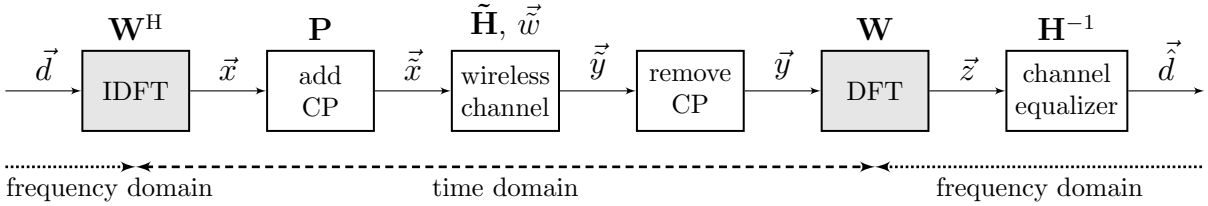

Figure 2.3: Block diagram of OFDM transceiver.

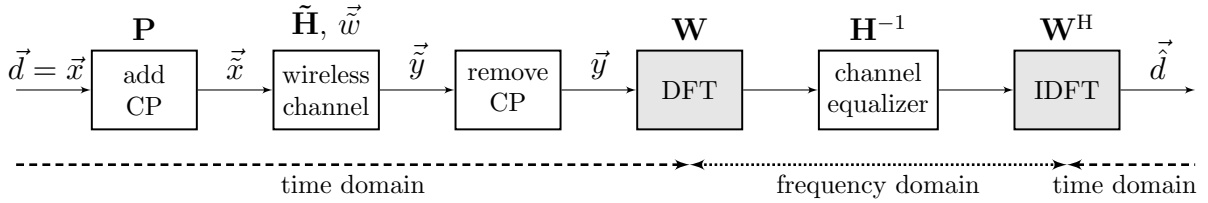

Figure 2.4: Block diagram of SC-FDE transceiver.

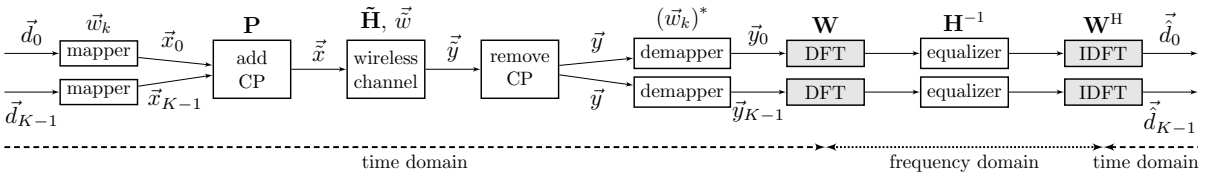

Figure 2.5: Block diagram of SC-FDM transceiver.

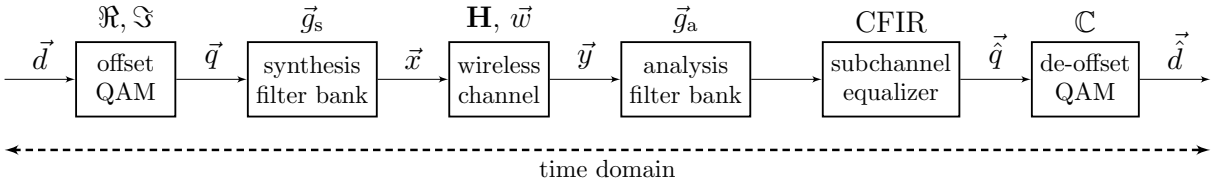

Figure 2.6: Block diagram of FBMC/OQAM transceiver.

the analysis filter bank with prototype filter $\vec{a}_{\mathrm{s}}$ is used to receive the signal. The channel is equalized in time domain for each subcarrier individually with a complex FIR filter based on a channel response $\vec{h}$ [IHSRR06, IILR11, SIVR10]. Lastly, OQAM modulation is reversed to obtain the received QAM symbols $\vec{\hat{d}}$.

2.3 Selected Transmission Scenarios

Looking at the history of mobile communications, each new generation of cellular systems has provided significant improvements over its predecessor. A common measure for the progress of technology in this area are the peak data rates. The most recent radio access standard, LTE, which is driven by the Third Generation Partnership Project (3GPP), can serve data rates in the order of Gbps. LTE-Advanced (LTE-A) is the first major improvement of LTE, which provides increased capacity and enhanced user experience. It

is specified in 3GPP Release 11 and is officially considered the fourth generation (4G) of cellular systems. With 3GPP Release 12, additionally the energy efficiency of the network and applications with diverse data requirements will be considered [ADF+13].
Extrapolating trends of the past two decades, in 5 years from now a new generation of cellular systems is anticipated. Besides expecting another leap in data rates, an additional aspect needs to be considered. Driven by the very success of cellular technology, advanced application scenarios evolve and pose new challenges that need to be addressed [Fet12, FA14]. One important question that must be answered is: What makes a system 5G? From a physical layer (PHY) point of view, the answer is flexibility. This includes techniques for spectral shaping of the transmitted signal, as well as adjustable partitioning of time and frequency resources, with the goal to be able to address different applications by adapting the parameters of a single waveform.
In the following, the three transmission scenarios illustrated in Figure 2.7 are presented, because they are particularly relevant for fifth generation (5G) systems.

Scenario A: Bitpipe Communication During the past few years, user behavior has developed beyond making calls and browsing websites on a mobile device. The trend is clearly directed towards exchanging content [Cis11] and sharing experiences. What used to be text based chat a few years ago is enhanced these days by embedded audio, image and video files. Live streams and television are broadcasted over Internet protocol (IP). Cloud storage for pictures and videos as well as music streaming services increasingly gain popularity and at the same time media formats evolve. For instance the 4K video resolution provides more than 8 million pixels in a single frame and new features like 3D television involve a multiple of that.
The requirements in this scenario are clearly an increased network capacity and higher data rates. Besides addressing this with improvements in the architecture of the network, these points are addressed in LTE with techniques like mulitple input multiple output (MIMO) [SBM+04], coordianted multi point (CoMP) [IDM+11] and spectrum aggregation [CCZY09]. From a physical layer perspective, to meet future demands, higher bandwidths and improved spectral efficiency will be mandatory. Additional techniques like dynamic spectrum access (DSA) [LCLM11] can support the strive to improve the utilization of vacant frequency resources. Spectral shaping will play a major role.

Scenario B: Low Latency Communication In the different stages of development of mobile communication, the purpose of cellular systems has also evolved. First, the goal was to transmit voice, then text messages arrived and now it transforms into delivering content to mobile devices. What lies ahead cannot be predicted with complete certainty, but at this point in time one vision for the future is directed towards a cellular network with significantly reduced latency [FBW+14], which can enable real-time interaction. For this objective, round trip delays of less than 1 ms are envisioned [Fet14]. While such a goal

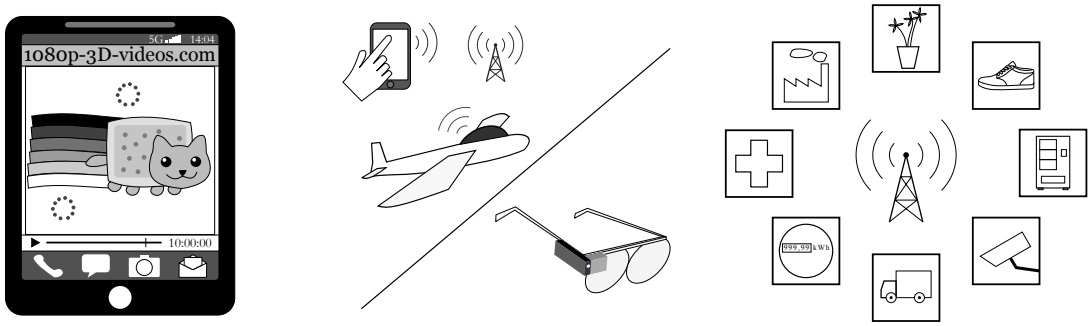

(a) Bitpipe Communication **(b)** Low-Latency Communication **(c)** Machine Type Communication

Figure 2.7: 5G application scenarios.

might appear very ambitious, if realized, it would enable new applications in areas like robotics and manufacturing, real-time traffic control, cellular gaming and virtual reality. To achieve 1 ms roundtrip delay, the time budget for the PHY cannot be larger than in the order of 100 μs and higher level protocols must support the goal of low latency. The current frame structure of LTE is based on symbols with duration of 70 μs, which leads to a latency at least one order of magnitude above the target. Low latency communication requires the transmission of short bursts and with high bandwidth, in combination with a frame structure that contains minimal overhead.

Scenario C: Machine Type Communication As cellular systems have made a major impact on people in the past, it is only natural that also machines are increasingly able to take advantage of wireless communication systems. In this context, the term Internet of Things (IoT) [AIM10] refers to objects being uniquely identified and connected via the Internet. As a subset of IoT, machine type communication (MTC) or machine-to-machine (M2M) communication does not have the purpose of human interaction but allows for devices to communicate directly with one another. Example areas include home automation, industrial monitoring, health care, agriculture and many other applications where collecting data can help optimize the outcome. In this context, the processing of large amounts of information, poses an additional challenge. The MTC market is not easily outlined, due to the enormous diversity of its applications. But exactly this potential makes cellular MTC interesting for mobile operators.
The requirements are quite different from providing a classical bitpipe. It can be expected, that in a few years from now, orders of magnitude more devices than people will be communicating, mostly sending or receiving small packets of either sensor or control data. Depeding on the application, there will be different classes of reliability, latency, security, mobility, etc. regarding the wireless connection and aspects like coverage and indoor penetration gain further significance [FDM+11, LSB+14]. Current applications tend to employ short range standards like Zig-Bee or revert to GSM. But sending measurement

data via SMS entails a large amount of protocol overhead. A 4G extension for MTC is already on the agenda for 3GPP Release 12 [ADF+13]. Beyond that, a future system has to provide an air interface with minimal hardware complexity and protocol overhead so that a considerably larger number of devices can be connected.

2.4 Conclusions

This chapter described common models for the wireless channel, in particular AWGN, frequency selective, time variant as well as a combined time-variant and frequency selective block fading model have been presented.
Further, it provided an overview of existing multicarrier techniques and reviewed the mathematical background of the prominent waveforms, i.e. OFDM, SC-FDE and FBMC. SC-FDM has been introduced as a frequency multiplexing version of SC-FDE.
Lastly, three transmission scenarios were addressed. A 'bitpipe communication' scenario, which demands a high spectral efficiency and increased throughput. A 'low latency' scenario with the goal to enable round-trip delays below 1ms. And 'machine type communication', which revolves around serving a multitude of terminals with diverse requirements regarding data rate, reliability, spectral and energy efficiency, etc.

Chapter 3

Basic GFDM Transmitter and Receiver

In this chapter, first the generic structure of a filtered multicarrier system is introduced. Therein, the modulator block defines the waveform and its characteristic properties, while the error rate performance of the transmission is mainly determined by the corresponding demodulator. Based on this, the details of generalized frequency division multiplexing (GFDM) signal generation and reception are explored, with the focus on a basic matched filter approach. Different representations of the signal processing are presented as an extension to the inital work on GFDM by the authors of [FKB09]. Further, as a generalized scheme, GFDM is related to the previously presented techniques orthogonal frequency division multiplexing (OFDM), single-carrier with frequency domain equalization (SC-FDE) and single-carrier frequency division multiplexing (SC-FDM). The goal is to show how a flexible reconfiguration can cover these three schemes as special cases. Lastly, an analysis of the performance of the system is conducted. For this purpose, the self-interference in GFDM is characterized as a random variable and based on this, an approximated analytic expression for the bit error rate (BER) is derived for additive white Gaussian noise (AWGN) channels. Moreover, calculated and simulated results are compared and Rayleigh multipath fading channels are considered.

3.1 Digital Baseband Transceiver Structure

Consider a generic baseband transmitter and a receiver with the structure depicted in Figure 3.1. At the beginning of the processing chain, a source provides the vector of binary data $\vec{b}$, which is subsequently passed to an encoder that operates with rate R to generate $\vec{b}_c$. A mapper, e.g. quadrature amplitude modulation (QAM), maps sequences of μ encoded bits to symbols from a 2^μ-valued complex constellation. The resulting vector $\vec{d}$ is referred as a data block and has N entries. The following baseband modulator block

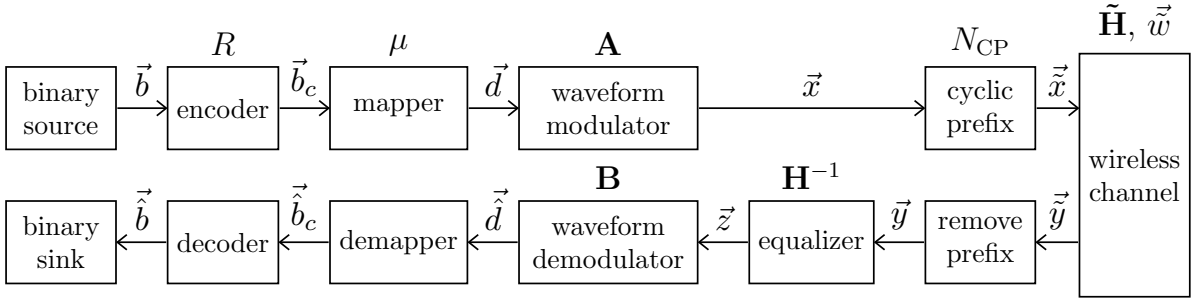

Figure 3.1: Generic block diagram of the transceiver.

yields the transmit samples $\vec{x}$, which are obtained by applying a pulse shape to each element of $\vec{d}$. Lastly, $\vec{x}$ is extended with a cyclic prefix (CP) by copying N_{CP} samples from the end of $\vec{x}$ to the beginning, which produces $\tilde{\vec{x}}$.
The wireless channel can be modelled according to (2.14) from Section 2.2.1. Adding a CP to the signal allows to simplify the model by replacing the linear convolution of the transmitted signal and the channel impulse response with a circular convolution.
The receiver acquires a vector of samples $\tilde{\vec{y}}$. At this point, it is assumed that transmitter and receiver operate synchronized in time and frequency. Similar to the transmitting counterpart, $\vec{y}$ denotes the signal after removing the CP. Given that the subsequent equalizer block has perfect channel knowledge available, it produces $\vec{z}$ by compensating the effects of the wireless channel. In the context of this work, considerations are made under the assumption of block fading, i.e. the channel response being time invariant for the duration of one block. The equalizer can perform either zero-forcing (ZF) as indicated in the diagram, or be the implementation of a metric like minimum mean squared error (MMSE). The equalized signal is then passed to the baseband demodulator to recover the transmitted data block, which yields $\hat{\vec{d}}$. Finally, the data symbols in $\hat{\vec{d}}$ are demapped, e.g. by a slicer, to produce a sequence of bits $\hat{\vec{b}}_{\mathrm{c}}$, which is then passed to a decoder to obtain $\hat{\vec{b}}$. An overview of the dimension of the relevant vectors is provided in Table 3.1.
The properties of the transmitted signal $\tilde{\vec{x}}$ depend on the algorithms implemented in the modulator block. But before discussing them in detail, it is helpful to define the structure of the data block $\vec{d}$.

Table 3.1: Size of relevant vectors.

Variable	Dimension	Comment
$\vec{b}, \hat{\vec{b}}$	$\mu RN \times 1$	number of uncoded bits
$\vec{b}_{\mathrm{c}}, \hat{\vec{b}}_{\mathrm{c}}$	$\mu N \times 1$	number of coded bits
$\vec{d}, \vec{x}, \vec{y}, \vec{z}, \hat{\vec{d}}$	$N \times 1$	number of data symbols/signal samples
$\tilde{\vec{x}}, \tilde{\vec{y}}$	$(N + N_{\mathrm{CP}}) \times 1$	number of samples including prefix

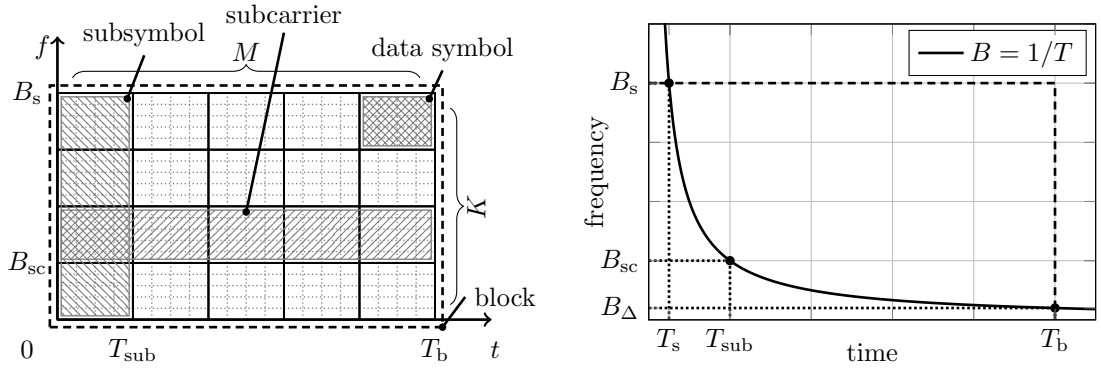

(a) Overview of GFDM block structure of and corresponding terminology.

(b) Time and frequency units within a GFDM block.

Figure 3.2: Relevant variables and parameters in the context of GFDM.

3.2 Block Structure

Transmitting and receiving data in quantities of blocks is a common concept in communication systems. In GFDM each block is designed to carry $N = KM$ complex valued data symbols, which are scattered across K subcarriers and M subsymbols. Figure 3.2(a) shows an example time-frequency grid, which is annotated with the terminology that will be used. The smallest unit in this context is a data symbol. A subcarrier consist of M data symbols which are transmitted consecutively, using multiple time slots on a specific center frequency. A subsymbol denotes K data symbols that are transmitted in the same time slot using multiple center frequencies in parallel.
Based on this data block definition and assuming a digital signal that is sampled with the frequency B_s, the time and frequency dimensions of the signal can be determined. First, the sampling period is calculated as

$$T_s = \frac{1}{B_s}. \tag{3.1}$$

Because there are K equidistant subcarriers in the system, the spacing between them is chosen as

$$B_{sc} = \frac{B_s}{K}. \tag{3.2}$$

Note that this definition allows to support orthogonal and non-orthogonal configurations with GFDM. If it is not desired to have the option for orthogonality, the subcarrier distance could be smaller. Moreover, B_{sc} is the distance between the subcarrier center frequencies and does not necessarily represent the actual bandwidth that is occupied by the subcarrier. The inverse of B_{sc} determines the duration of a subsymbol as

$$T_{sub} = \frac{1}{B_{sc}} = KT_s. \tag{3.3}$$

As previously established, there are M subsymbols in a block, hence the total block duration sums up to

$$T_\mathrm{b} = MT_\mathrm{sub} = NT_\mathrm{s}. \tag{3.4}$$

Lastly,

$$B_\Delta = \frac{1}{T_\mathrm{b}} = \frac{B_\mathrm{sc}}{M} \tag{3.5}$$

denotes the frequency gap between two samples of the signal in the frequency domain. Note that from (3.3) it follows that each subsymbol is represented by K samples in the time domain, while (3.5) shows that each subcarrier consists of M samples in the frequency domain.
The relation between bandwidths and durations is clarified in Figure 3.2(b). The variables and parameters characterizing the GFDM block are summarized in the appendix.

3.3 Baseband Processing

The waveform modulator determines if the tranceiver presented in the previous section produces a signal with GFDM or OFDM properties or even generates some other waveform. In the following, three approaches describing the signal processing in the modulator and the corresponding demodulator block will be presented. First, a model based on superposition of pulses will be given, which is useful for understanding the structures in the GFDM signal. Then a compact notation that is based on a compact matrix model will be introduced. Lastly, a signal description in frequency domain will be given, which is based on discrete Fourier transform (DFT) [OSB+89, pp.542-544] processing. This approach is particularly useful when considering a practical implementation of the algorithms.

3.3.1 Approach A: Superposition of Pulses

In this section, the GFDM modulation process is described in terms of filtering each individual data symbol with a corresponding pulse shape and then superpositioning all signal parts to obtain the transmit samples. The signal is processed in baseband. A structure that follows this approach is depicted in Figure 3.3. At the input of the modulator, let

$$d_n, \quad n = 0, \ldots, N-1 \tag{3.6}$$

be the elements of a GFDM data block. For the further description of the modulation process, it is useful to convert the symbol index n into a subcarrier index k and a subsymbol index m, which then allows to refer to the data symbols as

$$d_{k,m}, \quad k = 0, \ldots, K-1 \text{ and } m = 0, \ldots, M-1. \tag{3.7}$$

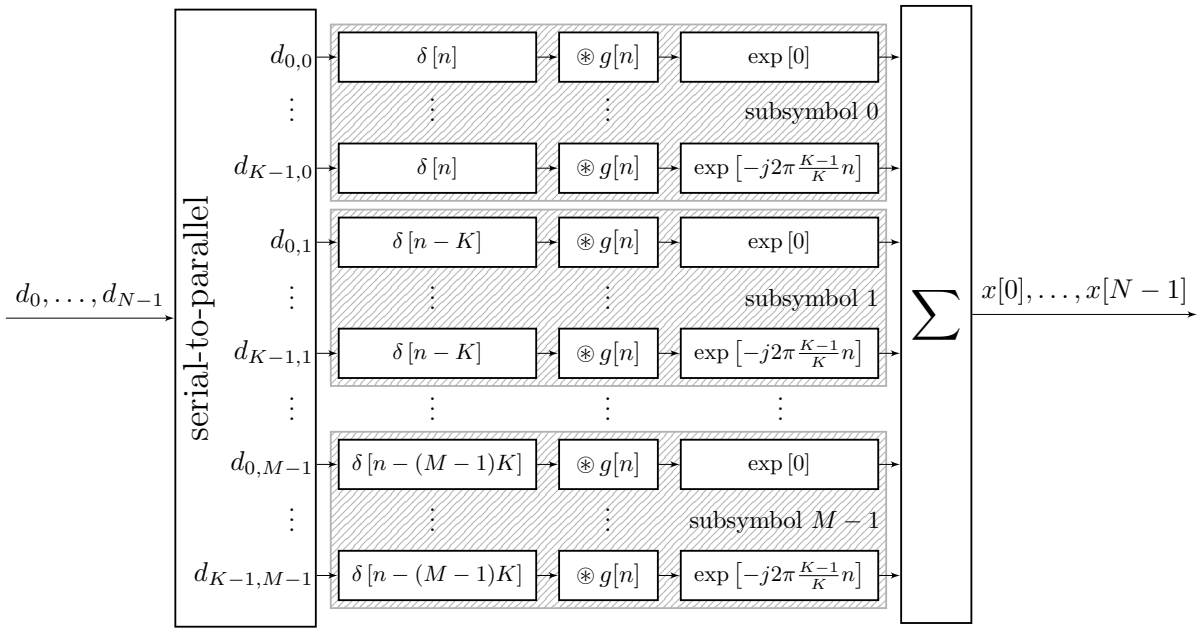

Figure 3.3: Block diagram of GFDM modulator.

Each $d_{k,m}$ corresponds to the data that will be transmitted on the kth subcarrier and in the mth subsymbol resource of the GFDM signal. In the block diagram, the serial-to-parallel conversion block also converts the notation from d_n to $d_{k,m}$. The indices n, k, and m are linked through $m = \left\lfloor \frac{n}{K} \right\rfloor$ and $k = n \bmod K$ in one direction and $n = mK + k$ in the other.

After this operation, the signal path splits into N parallel substreams. In each stream, the respective data symbol $d_{k,m}$ is multiplied with an impulse $\delta[n - mK]$, which has two effects. First, the substream signal is stuffed with $N - 1$ zeros, i.e. N times upsampling is performed. Here, it is necessary that $KM \leq N$, in order to meet the Nyquist criterion for all subcarriers in the system. Second, a time shift of mK samples is introduced, which moves each data symbol to the correct subsymbol position in the GFDM block. Subsequently, the signal is modulated with a prototype pulse shape $g[n]$ and multiplied with a complex exponential $e^{-j2\pi\frac{k}{K}n}$, which shifts the center frequency of the branch to address the K subcarriers in the system. It is important to note that the prototype pulse is defined with circularity $g[n] \equiv g[n \bmod N]$. Finally, the transmit samples $x[n]$ with sample index $n = 0, \ldots, N - 1$ are obtained through the superposition of all substream signals. The result of the modulation can be expressed as

$$x[n] = \sum_{k=0}^{K-1} \sum_{m=0}^{M-1} \left(d_{k,m} \cdot \delta[n - mK]\right) \underset{n,N}{\circledast} g[n] \cdot e^{-j2\pi\frac{k}{K}n}, \tag{3.8}$$

where $\underset{n,N}{\circledast}$ denotes circular convolution with respect to sample index n and with periodicity N.

The fact that circular convolution is used over regular convolution is a key property that defines GFDM. It is referred to as 'tail biting' [FKB09], a terminology borrowed from